Available online at www.sciencedirect.com
SCIENCE DIRECT®
ELSEVIER
European Journal of Mechanics B/Fluids 21 (2002) 657–675
EUROPEAN JOURNAL OF MECHANICS B/FLUIDS

The evolution of an initially circular vortex near an escarpment. Part I: analytical results ☆

D.C. Dunn [a,*,1], N.R. McDonald [b], E.R. Johnson [b]

[a] *Department of Aeronautics, Imperial College, Prince Consort Road, London SW7 2AZ, United Kingdom*
[b] *Department of Mathematics, University College London, Gower Street, London WC1E 6BT, United Kingdom*

Received 20 December 2001; accepted 26 August 2002

Abstract

The motion of a quasigeostrophic, equivalent-barotropic, initially circular vortex patch near an infinitely long topographic escarpment is studied using f-plane dynamics. There are two time scales in the problem: the advective time scale associated with the vortex, and the time scale for topographic vortex stretching. Analytical progress is possible when these two time scales are well-separated and results are presented here.

If topographic vortex stretching dominates advection by the vortex the vortex is said to be 'weak'. The vortex patch remains circular on the topographic time scale, and dispersive topographic waves rapidly propagate the initial disturbance away from the vicinity of the vortex. Subsequently cross-isobath motion is inhibited, and the vortex moves as though the escarpment were a plane wall. The same behaviour was observed for the motion of a weak singular vortex near an escarpment by Dunn, McDonald and Johnson [7], who named the phenomenon the 'pseudoimage' of the vortex.

If advection dominates over topographic effects, the vortex is said to be 'intense'. The vortex also remains circular to leading order, but the relative vorticity produced by the swirl of the vortex is less able to escape the vicinity of the vortex. The vortex follows a similar curved trajectory to those observed for intense vortices on the β-plane. The dipolar mechanism for this behaviour is described. Large time solutions are inhibited by the form of the escarpment topography, but examination of the equations leads to the conclusion that the leading order solution may be predict the motion for times beyond its formal range of validity.

Keywords: Vortex motion; Topography; Geophysical fluid dynamics

1. Introduction

There are regions in the deep ocean where, at least locally, the background gradient of potential vorticity is dominated by varying topography, rather than planetary curvature, or the β-effect as it is often represented in theoretical models. Of interest to the present study are regions of sharp topographic gradients such as the mid-Atlantic ridge, or the continental margins. In such regions the trajectories of eddies, such as those affecting the dispersal of newly-formed bottom water, are expected to depend, to leading order, on the local topographic gradients. See, for example, Stern [18], Beismann, Käse and Lutejeharms [2], Richardson and Tychensky [17] and McDonald [13]. Atmospheric eddies, such as tropical cyclones are also affected by

☆ This work was supported by NERC under grant GT4/95/206/M.
* Corresponding author.
E-mail address: d.c.dunn@bristol.ac.uk (D.C. Dunn).
[1] Present address: School of Mathematics, University of Bristol, University Walk, Bristol BS8 1TW, United Kingdom.

0997-7546/02/$ – see front matter
PII: S0997-7546(02)01208-6

sharp topographic gradients such as coastal mountain barriers. Given the potential damaged caused by cyclones impinging on inhabited areas, the calculation of their trajectories is an important meteorological question.

In two previous studies McDonald [14], and Dunn et al. [7] have investigated the motion of a singular vortex near an escarpment, using quasigeostrophic f-plane dynamics. Two time scales arise naturally in the problem, namely the time-scale for the vortex circulation, T_a, and the time-scale for topographic wave generation, T_w. McDonald [14] considered the case of an intense vortex, $T_a \ll T_w$, so that advection of fluid across the escarpment dominates over topographic wave generation. Under this assumption it was found that, initially, cyclones propagate away from the deep water region and anticyclones propagate away from the shallow water region. Asymptotic results showed that eventually cyclones and anticyclones propagate parallel to the escarpment at a speed that decays exponentially with the distance of the vortex from the escarpment. Moreover the drift speed always matches a possible topographic phase speed, and non-decaying topographic waves are radiated as a result. The vortex responds to this radiation by drifting slowly perpendicular to the escarpment. Provided that they are initially located within about a Rossby radius from the escarpment, cyclones accumulate at a distance of about 1.2 Rossby radii from the escarpment on the shallow side. Anticyclones exhibit similar behaviour except that they accumulate on the deep side of the escarpment.

The remaining cases of a weak vortex ($T_a \gg T_w$) and a moderate vortex ($T_a \approx T_w$) were considered by Dunn et al. [7]. For the weak vortex, linear theory predicts that, for times much shorter than T_a, the topographic waves rapidly propagate away from the vortex and have no leading order influence on its drift velocity. For times large compared to the topographic wave time scale the escarpment inhibits cross isobath motion of fluid, and the vortex moves as though it has an image in the escarpment, i.e., the escarpment acts like a wall. This phenomenon was named the *pseudoimage* of the vortex. Large time asymptotic results predict that when the vortex moves in the same direction as the topographic waves, non-decaying waves are radiated and the vortex drifts towards the escarpment as a result of this radiation. Weak vortices moving counter to the waves reach a steady drift velocity parallel to the escarpment. No theory is available for the case of a moderate vortex, but contour dynamics simulations show that dipole formation is a typical feature of the motion, and that moderate vortices experience enhanced drift perpendicular to the escarpment, in comparison to the weak vortex.

A limitation of the singular vortex model is the inability of the singular vortex to change its shape; the Bessel function structure of the singular vortex is preserved for all time, and so the velocity field associated with the vortex is always radially symmetric. Consequently the process of vortex deformation is absent in the singular vortex model, and this, in turn, has two implications regarding the ability of that model to describe the physical mechanisms of a more realistic vortex-topography interaction. First, the contribution of vortex deformation to the velocity field is excluded, so that a description of both the vortex drift and the advection of the ambient potential vorticity by the vortex is incomplete. Second, the possibility that the vortex responds to wave radiation by deforming is excluded. A more realistic model of vortex motion near an escarpment should examine the effects of vortex deformation on the evolving flow. In this paper the motion of an initially circular patch of uniform potential vorticity near an escarpment is investigated, and some analytical results for the cases of a weak and an intense vortex are given. Of particular interest is a comparison of the motion with the singular vortex model, i.e., how well does the singular vortex model describe the motion of the vortex patch centroid, and what features of the motion of the vortex patch model are absent in the singular vortex model? Subsequently, in Dunn [6] (hereinafter referred to as Part II), contour dynamics experiments will consider the accuracy of these results, as well as considering the case of a moderate intensity vortex.

As well as being important in its own right, the escarpment topography serves as a useful paradigm for the β-plane. In particular the direction going from deep to shallow water is analogous to the northwards direction on the β-plane, since both these directions are in the sense of increasing ambient potential vorticity. The evolution of a vortex patch on the β-plane has received considerable attention. The approach to the present problem is adapted from the now standard formulation of Sutyrin and Flierl [19], where the equation for the production of relative vorticity by advection of the ambient potential vorticity (the so-called "regular" field) is written in a form independent of vortex deformation. This latter effect (the "singular field") is then described by an equation forced by the leading order regular field. The particular formulation given below is adapted from that of Reznik, Grimshaw and Benilov [16], which explicitly includes an equation for the drift of the vortex centroid. A further work which has influenced the present study is that of Lam and Dritschel [11], in which the evolution of an initially circular vortex patch on the β-plane is investigated using the Contour Advective Semi-Lagrangian (CASL) algorithm of Dritschel and Ambaum [5].

The effect of the topography on the vortex is of primary interest, so the question of how the vortex came to be near the escarpment is ignored. It could have, for example, been carried by a background mean flow, or arrived due to the drift induced by the β-effect. In the following, it is assumed that no part of the vortex straddles the escarpment at the initial time, i.e., the vortex radius is less than the distance of the vortex centre from the escarpment. This assumption greatly simplifies the analysis.

The paper is organised as follows. First the leading order solution on the topographic wave time scale for a weak vortex patch is obtained by Fourier analysis. Second, the leading order solution for an intense vortex patch is obtained by the Green function method. Some aspects of the large-time behaviour of an intense vortex are deduced from the equations.

2. Problem formulation

Shallow water, quasi-geostrophic motion on the f-plane is governed by the conservation of potential vorticity, which can be written in non-dimensional form as

$$Q_t + J[\psi, Q] = 0, \tag{1}$$

where the conserved quantity is the quasigeostrophic potential vorticity,

$$Q = \nabla^2\psi - \psi + Sh_B(y). \tag{2}$$

Here ψ is the streamfunction, t is the time, $h_B(y)$ is the topography which is assumed to vary only in the y-direction and $J[f, g] = f_x g_y - g_x f_y$ is the Jacobian. The form of (2) implies that equivalent-barotropic dynamics are assumed. In the context of the present work this is an attempt to model the stratification of the abyssal ocean, i.e., a layer of dense fluid laying under a layer of less dense fluid, and where the the interface between the two layers is free to deform. The length scale, L, used in this non-dimensionalisation is the Rossby radius, $R_D = (g'D)^{1/2}/f$, where D is the average depth of the layer containing the vortex, g' is the acceleration due to the reduced gravity of the fluid and f is the Coriolis parameter. The non-dimensional time-scale is the eddy turnover or advective time-scale, $T_a = R_D/U$, where U is the typical vortex velocity due to geostrophy. The parameter S is given by

$$S = \frac{L/U}{\delta^{-1} f^{-1}} = \frac{\delta}{Ro} = \frac{T_a}{T_w}. \tag{3}$$

Here it has been anticipated that the topography will be discontinuous, and δ is the height of the topography as a fraction of the total depth. Hence $T_w = (f\delta)^{-1}$ is the time-scale for topographic wave generation (see Johnson [9]). The two numbers, δ and Ro are small parameters, but their ratio S may take the whole range of values. The Rossby number, Ro, is a function of the distance of the vortex from the escarpment; the absolute magnitude of the velocity induced by the swirl of the vortex is not the important velocity scale. Without changing its absolute amplitude, moving a vortex away from the escarpment has the effect of weakening its effect compared with topographic wave generation. Hence T_a is the advective time associated with the vortex *at the escarpment*. Given that lengths are non-dimensionalised on the deformation radius, there are three non-dimensional parameters: S, L, and the vortex radius, a. This parameter space may have many regions of distinct behaviour, so we take L and a to be O(1) and concentrate on investigating S. The time scale, T_a, can be estimated from the structure of the vortex. For example, in this study, this can be done using the Bessel function structure of the vortex patch.

In the absence of topography, solutions which have piecewise constant potential vorticity can be constructed. For a circular patch of anomalous potential vorticity, the streamfunction satisfies

$$\nabla^2\psi_0 - \psi_0 = -\alpha H(a - r), \tag{4}$$

where a is the patch radius, r is the radial distance from the vortex centre and $\alpha = \pm 1$ gives the sense of the circulation. For $\alpha > 0$ it is clockwise (anticyclonic) and for $\alpha < 0$ it is anticlockwise (cyclonic). The solution to (4) is well known, and is

$$\psi_0(r) = \begin{cases} \alpha - \alpha a K_1(a) I_0(r), & r \leqslant a, \\ \alpha a I_1(a) K_0(r), & r > a. \end{cases} \tag{5}$$

The angular velocity of the vortex is

$$b(r) = \frac{1}{r}\frac{\partial\psi_0}{\partial r} = \frac{1}{r}\begin{cases} -\alpha a K_1(a) I_1(r), & r \leqslant a, \\ -\alpha a I_1(a) K_1(r), & r > a. \end{cases} \tag{6}$$

A vortex patch of this type is taken as the initial condition. The topography is "switched on" near a pre-existing vortex at time $t = 0$. In a frame of reference with the origin attached to the vortex centroid (to be defined), the governing equation is

$$\frac{\partial}{\partial t}\left(\nabla^2\psi - \psi\right) + J\left[\tilde{\psi}, \nabla^2\psi - \psi\right] + S\frac{\partial h_B}{\partial y}\frac{\partial\psi}{\partial x} = 0, \tag{7}$$

where $\tilde{\psi} = \psi - uy + vx$ and $\mathbf{u} = (u, v)$ is the drift velocity of the vortex centroid $(x_c(t), y_c(t))$. The initial distribution of anomalous potential vorticity is

$$\Omega_0 = \nabla^2\psi_0 - \psi_0 = -\alpha H(a - r), \tag{8}$$

and so the total potential vorticity is

$$Q_0 = \Omega_0 + Sh_B(y). \tag{9}$$

The boundary between the two different values of Ω_0 represented in (8) by the Heaviside function is a material line and is advected with the flow, so subsequently the anomalous potential vorticity must have the form

$$\Omega = \nabla^2\psi - \psi = -\alpha H(r_0 - r) + q(x, y, t). \tag{10}$$

Here q is produced by redistribution of the ambient potential vorticity by the vortex, while $r_0 = r_0(\theta, t)$ is the equation of the evolving patch boundary. Substituting (10) into (7) and equating to zero the regular and singular parts in the resulting expression[2] leads to

$$\frac{\partial q}{\partial t} + J[\tilde{\psi}, q] + S\frac{\partial h_B}{\partial y}\frac{\partial \psi}{\partial x} = 0, \tag{11}$$

$$\frac{\partial r_0}{\partial t} + J[\tilde{\psi}, r_0 - r]|_{r=r_0} = 0. \tag{12}$$

These equations describe the two processes which contribute to the motion. The first equation, (11), describes the redistribution of ambient potential vorticity by the vortex. The second equation, (12), describes the deformation of the vortex $H(r_0 - r)$, which can be characterised entirely in terms of the motion of the boundary r_0.

The present choice of topography is

$$h_B(y) = \frac{\operatorname{sgn}(y)}{2}, \tag{13}$$

i.e., an infinite escarpment aligned along $y = 0$. By analogy with the β-plane, shallow water lies in the direction of increasing y. For convenience of description, the direction of increasing y is identified as north (or meridional), and increasing x as east (or zonal). In reality there is no preferred direction on the f-plane, so this choice is made simply to align the isobaths in the β-plane sense.

The fluid motion is strictly *not* quasigeostrophic near $y = 0$, since there the topography has infinite gradient, so the flow must be three-dimensional near the escarpment. However, the present choice of topography is an attempt to model a sudden depth change, ΔD, i.e., the horizontal length scale of the depth change (say l) is such that $R_D \gg l \gg \Delta D$. This implies that the vertical velocity scales like $\Delta D/l \ll 1$. It is assumed that the three-dimensional effects near the escarpment are negligible and have no leading order effect on the dynamics.

Johnson and Davey [10] have derived the dispersion relation for the linear topographic waves ($S \gg 1$) in this domain:

$$\omega = -\frac{Sk}{2\sqrt{k^2 + 1}}. \tag{14}$$

Hence the phase and group velocities are

$$c_p(k) = -\frac{S}{2\sqrt{k^2 + 1}}, \tag{15}$$

$$c_g(k) = -\frac{S}{2(k^2 + 1)^{3/2}}, \tag{16}$$

so that both the phase and energy of the waves propagate in the direction of decreasing x, i.e., with shallow water to the right. This paper considers the problem of an initially circular vortex located a distance L from the escarpment, as shown in Fig. 1.

To close the problem a definition of the vortex centroid is required. In the present case the geometric centroid is chosen (after [16,11]), which coincides with its centre of vorticity. This is not the only possible choice, since obtaining the solution in any coordinate frame yields all of the information about any characteristic point associated with the vortex. The centroid location $(x_c(t), y_c(t))$ is

$$x_c = \frac{\iint_V x\,\mathrm{d}x\,\mathrm{d}y}{\iint_V \mathrm{d}x\,\mathrm{d}y}, \qquad y_c = \frac{\iint_V y\,\mathrm{d}x\,\mathrm{d}y}{\iint_V \mathrm{d}x\,\mathrm{d}y}, \tag{17}$$

where V is the vortex patch bounded by the curve $r_0(\theta, t)$. Using Green's theorem these are, in polar coordinates,

[2] By which is meant the following. The Heaviside function leads to terms $\delta(r_0 - r)$ when substituted into the governing equation. The terms that are multiplied by the delta function are equated to zero and all remaining terms are similarly equated to zero. Hence the names "regular" and "singular", despite the fact that the equations are in fact both regular. This is standard practice for vortex patch analysis.

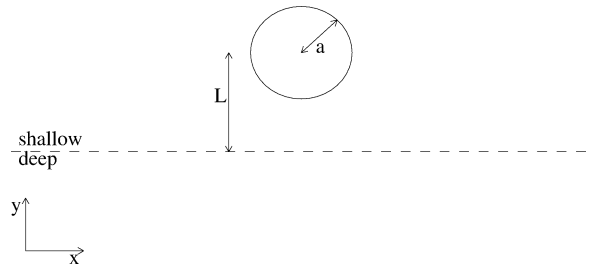

Fig. 1. The initial condition for the present problem. A circular patch of uniform relative vorticity of radius a is initially located with its centre distance L from the escarpment.

$$x_c(t) = \frac{1}{3\pi a^2}\int_0^{2\pi} r_0^3(\theta,t)\cos\theta\,\mathrm{d}\theta, \tag{18}$$

$$y_c(t) = \frac{1}{3\pi a^2}\int_0^{2\pi} r_0^3(\theta,t)\sin\theta\,\mathrm{d}\theta. \tag{19}$$

Here, the fact that the area of the patch, πa^2, is conserved, has been used. In the moving frame, $x_c(t) = y_c(t) = 0$, so the problem is closed by the condition

$$\int_0^{2\pi} r_0^3\,\mathrm{e}^{\mathrm{i}\theta}\,\mathrm{d}\theta = 0. \tag{20}$$

Eqs. (11), (12) and (20), together with the initial conditions,

$$\psi(r,\theta,0) = \psi_0(r), \tag{21}$$

$$q(x,y,0) = 0, \tag{22}$$

$$r_0(\theta,0) = a, \tag{23}$$

$$\big(x_c(0), y_c(0)\big) = (0,L), \tag{24}$$

describe the evolution of the vortex patch. A complete study of the problem requires consideration of the dependence of the motion on S, a and L, potentially a complicated parameter space. In the present paper a and L are taken to be O(1) and attention is focused on the effect of varying S. The leading order solutions for $S \gg 1$ (a weak vortex) and for $S \ll 1$ (an intense vortex) are obtained analytically, and are valid for $a < L$, so that the vortex patch does not initially intersect the escarpment. In Part II, the full range of values of S will be investigated using contour dynamics, including a validation of the results given here.

3. A weak vortex patch

For a weak vortex, $S \gg 1$, set $\varepsilon = S^{-1}$ and introduce the stretched time variable $\tau = t/\varepsilon$, so that the unit of time is T_w, the topographic wave time scale. Under this rescaling, Eqs. (11) and (12) become

$$\frac{\partial q}{\partial \tau} + \varepsilon J[\tilde{\psi}, q] + \frac{\partial h_B}{\partial y}\frac{\partial \psi}{\partial x} = 0, \tag{25}$$

$$\frac{\partial r_0}{\partial \tau} + \varepsilon J[\tilde{\psi}, r_0 - r]|_{r=r_0} = 0, \tag{26}$$

which express the fact that advection is O(ε) on this time scale. In particular, for times $\tau \ll \varepsilon^{-1}$, deformation of the patch boundary, is O(ε), so that r_0, can be taken to be constant, at least on the topographic wave time scale. The leading order solution to this problem is obtained by Fourier analysis.

For times $\tau \ll \varepsilon^{-1}$, ignoring the advection terms in (25) and (26) yields

$$\frac{\partial q}{\partial \tau} + \frac{\partial h_B}{\partial y}\frac{\partial \psi}{\partial x} = 0, \tag{27}$$

$$r_0 = a. \tag{28}$$

Eqs. (28) and (8) imply that the anomalous potential vorticity, (10), must have the form $\Omega = \nabla^2\psi_0 - \psi_0 + q(x, y, t)$. Hence the secondary circulations can be obtained by writing

$$\psi = \psi_0 + \phi. \tag{29}$$

The magnitude of the regular field ϕ can be O(1) or greater since $S \gg 1$ is the magnitude of the relative vorticity, q, acquired by a fluid particle crossing the escarpment. Substituting this into (10), with $r_0(\theta, \tau) = a$ for all τ, leads to

$$q = \nabla^2\phi - \phi. \tag{30}$$

As a matter of mathematical brevity, the solution is derived in the inertial frame of reference. Eq. (27) becomes the forced topographic wave equation,

$$\frac{\partial}{\partial \tau}\left(\nabla^2\phi - \phi\right) + \frac{\partial h_B}{\partial y}\frac{\partial \phi}{\partial x} = -\frac{\partial h_B}{\partial y}\frac{\partial \psi_0}{\partial x}. \tag{31}$$

This problem is very similar to the weak singular vortex problem of Dunn et al. [7], and may be solved in precisely the same fashion. The problem for ϕ is

$$\nabla^2\phi - \phi = 0, \quad y \neq 0; \tag{32}$$

$$\phi(x, y, 0) = 0, \quad \tau = 0; \tag{33}$$

$$\nabla\phi \to 0, \quad x^2 + y^2 \to \infty; \tag{34}$$

$$[\phi] = 0, \quad y = 0; \tag{35}$$

$$[\phi_{y\tau}] + \phi_x = -\psi_{0x}, \quad y = 0. \tag{36}$$

Here $[\,\cdot\,]$ denotes the jump of the enclosed quantity at $y = 0$. The governing equation (32) arises since the topography is flat everywhere except at $y = 0$, so $\partial h_B/\partial y = 0$ away from the escarpment. Condition (34) is the condition that the fluid is at rest far from the escarpment; condition (35) is continuity of surface elevation (or equivalently pressure) at the escarpment; (36) is obtained by integrating the governing equation (31) by parts across the escarpment (see [10]).

This differs from the weak singular vortex problem only in the form of the forcing term ψ_{0x} in the right-hand side of (36). Since a circular vortex does not contribute to its own drift, the advection of the vortex centre (x_c, y_c) is due to the regular field, i.e., the vortex drift velocity components are

$$\frac{\mathrm{d}x_c}{\mathrm{d}\tau} = -\varepsilon\phi_y|_{x=x_c, y=y_c}, \tag{37}$$

$$\frac{\mathrm{d}y_c}{\mathrm{d}\tau} = \varepsilon\phi_x|_{x=x_c, y=y_c}. \tag{38}$$

Hence, for times up to $\tau = \mathrm{O}(\varepsilon^{-1})$, $x_c = \mathrm{O}(\varepsilon)$ and $y_c = L + \mathrm{O}(\varepsilon)$, and the vortex term is, to leading order

$$\psi_0 = \psi_0(x, y - L). \tag{39}$$

The leading order solution is obtained by standard Fourier analysis. Denote the Fourier transform of ϕ by

$$\hat{\phi}(k) = \int_{-\infty}^{\infty} \phi\, \mathrm{e}^{-\mathrm{i}kx}\, \mathrm{d}x. \tag{40}$$

In Fourier space (32), (34) and (35) are

$$\hat{\phi}_{yy} - \left(k^2 + 1\right)\hat{\phi} = 0, \quad y \neq 0, \tag{41}$$

$$\hat{\phi} \to 0, \quad y \to \pm\infty, \tag{42}$$

$$\left[\hat{\phi}\right] = 0, \quad y = 0, \tag{43}$$

with solutions of the form

$$\hat{\phi} = B(k, \tau)\, \mathrm{e}^{-\sqrt{k^2+1}|y|}. \tag{44}$$

The matching condition (36), together with the initial condition (33), gives the initial value problem for B,

$$2\sqrt{k^2+1}B_\tau - \mathrm{i}kB = -\mathrm{i}k\hat{\psi}_0|_{y=0}, \tag{45}$$

$$B(k,0) = 0. \tag{46}$$

For $L > a$, so that no part of vortex patch crosses the escarpment,[3] the forcing term evaluated at the escarpment is,

$$\psi_0(x,0) = \alpha a I_1(a) K_0\big(\big(x^2+L^2\big)^{1/2}\big). \tag{47}$$

Making use of an identity from Gradshteyn and Rhyzik [8, p. 498], the Fourier transform of this is

$$\hat{\psi}_0|_{y=0} = \frac{\alpha a I_1(a)\pi}{\sqrt{k^2+1}}\,\mathrm{e}^{-|L|\sqrt{k^2+1}}. \tag{48}$$

Substitution of this expression in (45) gives

$$B_\tau + \mathrm{i}\omega B = -\frac{\alpha a I_1(a)\omega\pi}{\sqrt{k^2+1}}\,\mathrm{e}^{-|L|\sqrt{k^2+1}}, \tag{49}$$

with solution

$$B(k,\tau) = \frac{\alpha a I_1(a)\pi}{\sqrt{k^2+1}}\,\mathrm{e}^{-|L|\sqrt{k^2+1}}\big(\mathrm{e}^{-\mathrm{i}\omega\tau} - 1\big), \tag{50}$$

where

$$\omega = -\frac{1}{2\sqrt{k^2+1}}, \tag{51}$$

is the frequency of the topographic waves in the stretched time variable (cf. the dispersion relation in Eq. 14). The solution for the regular field consists of a steady term and a topographic wave term,

$$\phi = \phi^{(s)} + \phi^{(w)}, \tag{52}$$

where

$$\phi^{(s)} = -\alpha a I_1(a) K_0\big(\big(x^2 + \big(|y|+|L|\big)^2\big)^{1/2}\big), \tag{53}$$

$$\phi^{(w)} = \alpha a I_1(a)\int_0^\infty A(k,y)\cos(kx-\omega\tau)\,\mathrm{d}k, \tag{54}$$

with

$$A(k,y) = \frac{\mathrm{e}^{-(|y|+|L|)\sqrt{k^2+1}}}{\sqrt{k^2+1}}. \tag{55}$$

The topographic wave term is identical with the topographic wave term for the weak singular vortex solution of Dunn et al. [7], with the exception of the factor before the integral; hence by the same arguments used in that paper it immediately follows that the waves decay like $\tau^{-1/3}$ at the wavefront and like $\tau^{-1/2}$ in the wave train. Importantly, the waves decay rapidly, like τ^{-1}, at the x-location of the vortex centre, and so have no influence on the drift of the vortex as $\tau \to \infty$. Fig. 2 illustrates the solution (54) calculated using Fast Fourier Transforms. Note the features of a dispersive wave train: the largest amplitude disturbance is at the head of the wave train, and this decays exponentially ahead of the train. See Whitham [20] for details of the analysis.

Consider the steady part of the solution, $\psi_0 + \phi^{(s)}$. For $\mathrm{sgn}(y) = -\mathrm{sgn}(L)$, (i.e., across the escarpment from the vortex) the fluid is at rest. On the other hand for $\mathrm{sgn}(y) = \mathrm{sgn}(L)$ (on the same side of the escarpment as the vortex), the fluid behaves as if there were an equal and opposite circular patch of relative vorticity centred at $(0,-L)$, i.e., as if the escarpment were a plane wall. This phenomenon of the weak vortex 'thinking' that the escarpment is a wall is precisely the same as that found in Dunn et al. [7] for a weak singular vortex, and was named the *pseudoimage*. On the fast topographic wave time scale, this pseudoimage remains circular to within values of $\mathrm{O}(\varepsilon)$.

[3] This is consistent with the idea described in the introduction that the vortex has approached the escarpment from elsewhere. Without this assumption the Fourier transform of the forcing is more difficult.

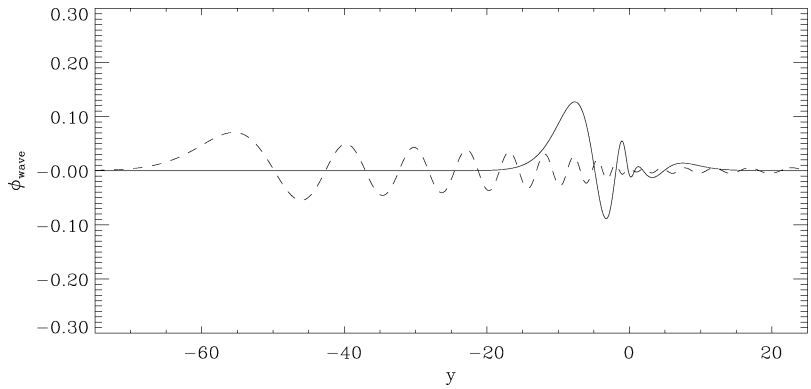

Fig. 2. The topographic wave term $\phi^{(w)}$ evaluated over $y = 0$ at times $\tau = 10$ (solid line) and $\tau = 60$ (dotted line). The parameter values used are $\alpha = 1$, $a = 1$ and $L = 1.2$.

The role of the pseudoimage in the study by Dunn et al. [7] was crucial. In the contour dynamics investigations to be described in Part II, it will be seen that the behaviour of the weak vortex patch is well predicted, for many eddy turnover times, by assuming that the escarpment is a wall. The evolution of a vortex patch near a wall is itself difficult to treat analytically,[4] but nevertheless the pseudoimage theory appears robust, and valid far beyond times for which it is formally valid. In the theory presented here the pseudoimage has a definite physical meaning. It is part of the topographic wave train, a wave train which is initially excited by the circulation of the vortex pushing fluid across the escarpment. It is non-dispersive and remains localised near the vortex. The magnitude of the relative vorticity associated with the disturbance $\phi^{(s)}$ is precisely that required to advect the vortex as if the escarpment were a plane wall. Since the dispersive topographic waves rapidly propagate away from the vortex, advection of the vortex is due solely to its pseudoimage as $\tau \to \infty$.

The vortex drift velocity components as $\tau \to 0$, obtained from Eqs. (37) and (38), via a leading order expansion of the solution (53) and (54) are

$$u = 0, \qquad v = \varepsilon\alpha a I_1(a)\tau \int_0^\infty \omega A(k, L)\,\mathrm{d}k, \tag{56}$$

while as $\tau \to \infty$, the advection of the vortex centre is solely due to the pseudoimage, giving

$$u = \varepsilon\alpha a I_1(a) K_1\big(2|L|\big)\operatorname{sgn} L, \qquad v = 0. \tag{57}$$

The integral in (56) converges, since $|A(k, y)| < \mathrm{e}^{-k}$, and is negative. Hence, for $\tau \ll 1$ the vortex moves with constant velocity in the y-direction. Cyclones ($\alpha < 0$) drift north and anticyclones ($\alpha > 0$) drift south, the same short-time behaviour as a weak singular vortex and the mechanism is precisely the same.

To understand the physical mechanism responsible for the drift of the vortex, consider Fig. 3. This plot shows the evolution of the streamlines associated with the regular solution, $\psi = \phi^{(s)} + \phi^{(w)}$ for a weak vortex patch for $\alpha = -1$, i.e., an anticyclone. In Fig. 3(a), the streamlines of (52) are plotted at $\tau = 0^+$. The initial response to the advection of fluid across the escarpment by the swirl velocity of the vortex is the establishment of a secondary dipole, centred over the escarpment and with its axis aligned along the y-axis. This is the result of the anticyclone drawing fluid to its west from the deep side of the escarpment, and pushing fluid to its east away from the shallow side of the escarpment. The vortex moves south along the dipole axis. This is the same initial response for an intense vortex near an escarpment *and* on a β-plane. In those cases however the strong circulation of the vortex rotates the dipole axis before the initial disturbance can disperse as topographic waves, causing the southwest (northwest) curved trajectories for anticyclones (cyclones). The meridional drift is not clear on the scale of the plot, and is only predicted in the limit $t \to 0$. The important point is that initialising the vortex at $t = 0$ displaces the potential vorticity interface, and provides a mechanism for the generation of a topographic wave train. This process is clear in Figs. 3(b) and 3(c), which show the rapid westward propagation of the topographic waves, away from the vortex centre. The final frame, Fig. 3(d), shows that as $\tau \to \infty$ only the solitary non-propagating disturbance (the pseudoimage) remains. The relative vorticity of the pseudoimage is $\mathrm{O}(\varepsilon^{-1})$, and is precisely strong enough to advect the weak primary vortex as if the escarpment were a wall. Thus, the weak

[4] There are a class of steadily propagating solutions, the so-called *V-states*, of Pierrehumbert [15]. In the terminology of the present work these are circular for $a \ll L$ and approach the singular vortex solution in the limit $a/L \to 0$.

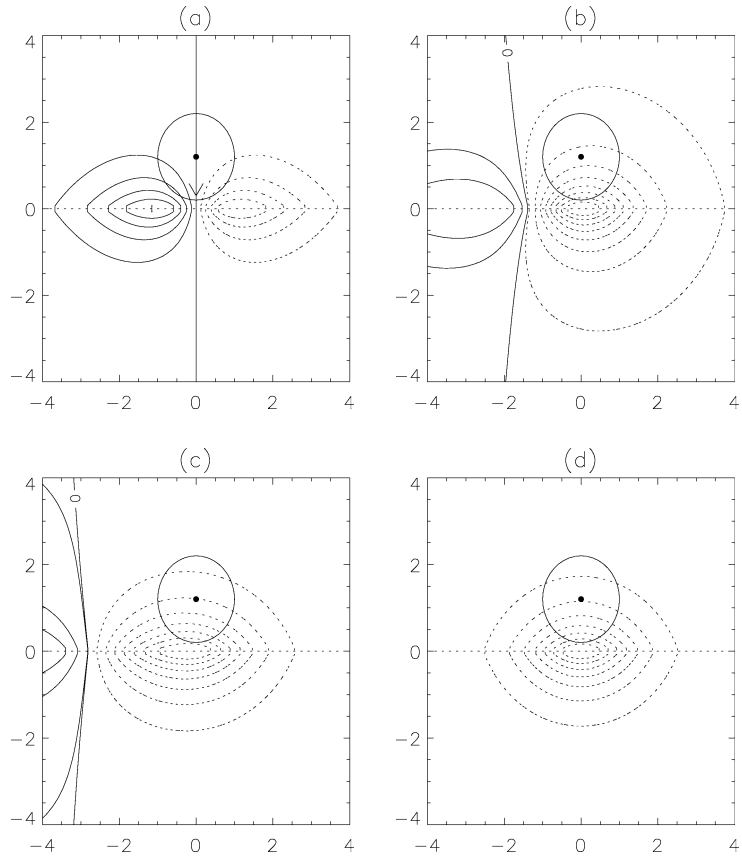

Fig. 3. The advection of the vortex, here an anticyclone, by the regular field. (a) Evaluation of ϕ at $\tau = 0^+$. Note that the initial advection is south, along the dipole axis. (b) ϕ evaluated at $\tau = 4$ and (c) evaluated at $\tau = 7$, from Eq. (52), (d) is the pseudoimage term, the regular field as $\tau \to \infty$. The vortex is shown by the circle and its centre by the dot. The parameter values used are $a = 1$, $\alpha = -1$ and $L = 1.2$. The solid (respectively dashed) lines indicate positive (negative) contour values. The 'tongue' moving away to the left is the topographic waves.

cyclones move east (west) when located on the shallow (deep) side of the escarpment and anticyclones drift west (east) when located on the shallow (deep) side of the escarpment.

The results of this subsection could have been obtained by replacing the vortex patch by a singular vortex of strength

$$\Gamma = \frac{\alpha a I_1(a)}{2\pi}, \tag{58}$$

initially located at $(0, L)$. That is, for as long as the theory is valid, the motion of a weak vortex patch is adequately modeled by the linear theory for a weak singular vortex. This is to be expected, since the flow exterior to a circular vortex patch is identical to that of a singular vortex. Formally, linear theory is only valid on the topographic wave time scale, i.e., $t = \mathrm{O}(\varepsilon)$ and for as long as the vortex patch remains circular. Further analysis is possible if the vortex patch is assumed to remain circular for times $t = \mathrm{O}(1)$. Such an approach is reasonable for $a \ll L$, but amounts to little more than modeling the vortex patch by a singular vortex. Moreover, west-traveling vortex patches (i.e., shallow water anticyclones and deep water cyclones) travel at a speed matching a possible topographic wave phase speed, and wave radiation must be important at large times. This process is expected to alter the shape of the vortex as it loses energy to the radiated waves. Since the effect of vortex shape changes is of particular interest in the present study, the large time behaviour will be examined by contour dynamics in Part II.

4. An intense vortex patch

The analysis in this section is based on that of Reznik et al. [16] and McDonald [14]. In the case of an intense vortex, $S \ll 1$ is a small parameter. To reformulate the problem note that the secondary circulations scale like S, and seek a solution to (11) and (12) in the form

$$\psi(r,\theta,t) = \psi_0(r) + S\phi_1 + \cdots, \tag{59}$$

$$q = Sq_1 + S^2 q_2 + \cdots, \tag{60}$$

$$r_0 = a + Sr_1 + \cdots, \tag{61}$$

$$(u,v) = S(u_1,v_1) + \cdots. \tag{62}$$

The initial conditions (21)–(24) become, for the leading order quantities,

$$\phi_1 = q_1 = r_1 = u_1 = v_1 = 0, \qquad t = 0. \tag{63}$$

The leading order solution, obtained below is valid for $t < \mathrm{O}(S^{-1})$. Substitution of (60) into (11) gives the initial-value problem for the leading order term in the expansion for the anomalous potential vorticity,

$$\frac{\partial q_1}{\partial t} + b(r)\frac{\partial q_1}{\partial \theta} = -b(r)\frac{\partial h_B}{\partial \theta}, \tag{64}$$

$$q_1(r,\theta,t) = 0, \tag{65}$$

where $b(r)$ is the angular velocity of the initial vortex, given by (6). Hence changes in the leading order potential vorticity anomaly is due to redistribution by the axisymmetric circulation of the primary vortex. Eq. (64) is easily solved by the method of characteristics. The complementary function is

$$\tilde{q_1} = \tilde{q_1}\big(\theta - b(r)t, r\big), \tag{66}$$

and the particular integral is

$$p(r,\theta) = -\frac{1}{2}\operatorname{sgn}(r\sin\theta + y_c), \tag{67}$$

since $h_B = \operatorname{sgn}(r\sin\theta + y_c)/2$ in the moving polar coordinate frame. The initial condition (65) leads to

$$\tilde{q_1}(r,\theta) = \frac{1}{2}\operatorname{sgn}\big(r\sin\big(\theta - b(r)t\big) + L\big), \tag{68}$$

so that the solution for the leading order vorticity correction is

$$q_1 = \frac{1}{2}\big[\operatorname{sgn}\big(r\sin(\theta - bt) + L\big) - \operatorname{sgn}\big(r\sin\theta + y_c\big)\big]. \tag{69}$$

Apart from the additional factor of $1/2$ (due to the particular choice of representation for the escarpment topography), this is formally the same as the leading order vorticity correction obtained by McDonald [14], differing only in the form of the angular velocity $b(r)$.

The equations governing the next order quantities are

$$\nabla^2\phi_1 - \phi_1 = q_1(r,\theta,t), \tag{70}$$

$$\frac{\partial r_1}{\partial t} + b(a)\frac{\partial r_1}{\partial \theta} + \frac{\partial \phi_1}{\partial \theta}(a,\theta,t) + u_1 a\cos\theta + v_1 a\sin\theta = 0, \tag{71}$$

$$\int_0^{2\pi} r_1(\theta,t)\,\mathrm{e}^{i\theta}\,d\theta = 0, \tag{72}$$

$$\frac{\partial q_2}{\partial t} + b(r)\frac{\partial q_2}{\partial \theta} = -J[\phi_1 + u_1 y - v_1 x, q_1] - J[\phi_1, h_B]. \tag{73}$$

The piecewise constant form of the vorticity correction, q_1, appearing as a forcing term in the equation for the streamfunction correction ϕ_1 in (70), inhibits progress. To proceed, it is assumed that the response for short times is dominated by azimuthal mode-1, since, according to Eq. (71), the leading order vortex drift velocity components (u_1, v_1) are controlled by this dipolar mode. This is analogous to the motion of an intense vortex on the β-plane where the mode-1 component is the well-known β-gyres.

First, writing

$$r_1(\theta,t) = r_1^{(s)}(t)\sin\theta + r_1^{(c)}(t)\cos\theta, \tag{74}$$

and substituting into (72), leads to

$$r_1 = 0, \tag{75}$$

i.e., the patch boundary remains circular to this order of approximation.

It is straightforward to obtain the azimuthal mode-1 Fourier coefficients for q_1. The derivation is given in Appendix A, and the result is quoted here:

$$q_1 = q_1^{(s)}(r,t)\sin\theta + q_1^{(c)}(r,t)\cos\theta, \tag{76}$$

where, for $r > |L|$,

$$q_1^{(s)} = \frac{2}{\pi r}\sqrt{r^2 - L^2}(\cos bt - 1), \tag{77}$$

$$q_1^{(c)} = -\frac{2}{\pi r}\sqrt{r^2 - L^2}\sin bt, \tag{78}$$

and, importantly, for $r < |L|$

$$q_1^{(c)} = q_1^{(s)} = 0. \tag{79}$$

In obtaining this approximation it has been assumed that $y_c = L + \mathrm{O}(S)$. Details can be found in Appendix A. This solution implies that $r = |L|$ defines a region which the leading order, dipole component of the redistributed ambient potential cannot enter. This is apparent in the contour dynamics simulations in Part II: the deflected topographic contour remains isolated from the vortex boundary. Note that q_1 is continuous at $r = |L|$.

Next, seeking a solution to (70) in the form

$$\phi_1(r,\theta,t) = \phi_1^{(s)}(r,t)\sin\theta + \phi_1^{(c)}(r,t)\cos\theta, \tag{80}$$

leads to

$$\left(\frac{\partial^2}{\partial r^2} + \frac{1}{r}\frac{\partial}{\partial r} - \left(\frac{1}{r^2} + 1\right)\right)\phi_1^{(\nu)} = q_1^{(\nu)}, \tag{81}$$

where the superscript (ν) can be either (s) or (c) for the sin or cos components, respectively. The Greens function for the operator in the left-hand side of (81), that is regular at the origin is well known (see, e.g., [19,11]), and is

$$G(r|\rho) = \begin{cases} -\rho I_1(r)K_1(\rho), & r < \rho, \\ -\rho K_1(r)I_1(\rho), & r > \rho; \end{cases} \tag{82}$$

so that

$$\phi_1^{(\nu)} = \int_0^\infty G(r|\rho)q_1^{(\nu)}\,\mathrm{d}\rho, \tag{83}$$

or, rather less appealing,

$$\phi_1^{(\nu)} = \begin{cases} -I_1(r)\displaystyle\int_{|L|}^\infty \rho q_1^{(\nu)}(\rho,t)K_1(\rho)\,\mathrm{d}\rho, & \text{if } r < |L|, \\ -I_1(r)\displaystyle\int_r^\infty \rho q_1^{(\nu)}(\rho,t)K_1(\rho)\,\mathrm{d}\rho - K_1(r)\int_{|L|}^r \rho q_1^{(\nu)}(\rho,t)I_1(\rho)\,\mathrm{d}\rho, & \text{if } r > |L|. \end{cases} \tag{84}$$

Note that the solution is continuous on $r = |L|$. Now, according to (75), Eq. (71) becomes

$$\frac{\partial\phi_1}{\partial\theta}(a,\theta,t) + u_1 a\cos\theta + v_1 a\sin\theta = 0. \tag{85}$$

But,

$$\frac{\partial\phi_1}{\partial\theta} = \phi_1^{(s)}\cos\theta - \phi_1^{(c)}\sin\theta, \tag{86}$$

in turn implying that

$$u_1 a = -\phi_1^{(s)}(a,t), \tag{87}$$

$$v_1 a = \phi_1^{(c)}(a,t). \tag{88}$$

Again, the constraint $a < |L|$ is adopted, i.e., the vortex patch does not initially cross the escarpment. The vortex drift velocity components are then

$$u_1 = \frac{2}{\pi a} I_1(a) \int_{|L|}^{\infty} (\cos bt - 1) K_1(r) \sqrt{r^2 - L^2}\, \mathrm{d}r, \tag{89}$$

$$v_1 = \frac{2}{\pi a} I_1(a) \int_{|L|}^{\infty} \sin bt\, K_1(r) \sqrt{r^2 - L^2}\, \mathrm{d}r. \tag{90}$$

These are the *same* expressions obtained by McDonald [14] for an intense singular vortex near an escarpment, except for the constant multiplying the integrals, and the particular form for the vortex angular velocity $b(r)$. Moreover, as $a \to 0$, $I_1(a)/a \to 1/2$, so the singular vortex drift velocity components are recovered from (89) and (90) in this limit.

The asymptotic behaviour of the integrals is derived in Appendix B and is quoted here. As $t \to 0$,

$$u_1 \approx -\frac{A\alpha^2 a I_1^3(a)}{2\pi} t^2, \tag{91}$$

$$v_1 \approx -\frac{B\alpha I_1^2(a)}{\pi} t, \tag{92}$$

where A and B are positive constants which depend on L. For $t \gg 1$ but less than $\mathrm{O}(S^{-1})$

$$u_1 \approx -\frac{2I_1(a)}{a} \exp\bigl(-|L|\bigr) + \mathrm{O}\left(\frac{\log^2 t}{t}\right), \tag{93}$$

$$v_1 \approx \mathrm{O}\left(\frac{\log^2 t}{t}\right). \tag{94}$$

In (91), (92), $\operatorname{sgn}(v) = -\operatorname{sgn}(\alpha)$ and $\operatorname{sgn}(u) = -1$, so at short times anticyclones ($\alpha > 0$) move south and west, while cyclones ($\alpha < 0$) move north and west. Eqs. (93), (94) indicate that after the initial meridional acceleration there is a slow decay in the meridional velocity. The zonal drift approaches the steady westward speed of $2SI_1(a)\exp(-|L|)/2a$. These features are clear in Fig. 4, which shows plots of the drift velocity components, and the centroid trajectory for a cyclone with $a = 1$ (solid line) and $a = 0.5$ (dotted line). Note that the smaller vortex experiences increased meridional drift and decreased zonal drift.

This behaviour is qualitatively that of an intense vortex on the β-plane.[5] The mechanism for this behaviour is illustrated in Fig. 5, which shows the evolution of the streamlines calculated from (83). Initially the vortex (here a cyclone) pushes fluid columns lying to its west (respectively east) from the shallow (deep) side of the escarpment to the deep (shallow) side. Potential vorticity conservation demands that these fluid columns acquire net cyclonic (anticyclonic) relative vorticity. This secondary dipole is initially symmetric about $x = 0$, as can be seen in Fig. 5(a), and results in an initial northwards drift of the cyclone. This is the same initial behaviour seen above for the weak vortex. However in the weak vortex case the topographic waves propagate the initial disturbance rapidly away from the vortex. In the intense vortex case the vortex time scale is much shorter than the topographic wave time scale and the initial disturbance remains localised in the vicinity of the vortex. Figs. 5(b) and 5(c) show that the strong cyclonic circulation of the vortex rotates the secondary dipole anticlockwise, which results in the vortex following the curved northwest trajectory. At large times, Fig. 5(d), the flow in the vicinity of the vortex approaches a uniform westward stream.

The flow near the dipole axis is approximately uniform: the residual flow ϕ_{res} is

$$\phi_{\mathrm{res}} = \phi_1 + u_1 r \sin\theta - v_1 r \cos\theta = \left[\phi_1^{(s)}(r,t) - \frac{r}{a}\phi_1^{(s)}(a,t)\right]\sin\theta + \left[\phi_1^{(c)}(r,t) - \frac{r}{a}\phi_1^{(c)}(a,t)\right]\cos\theta. \tag{95}$$

The coefficients of $\sin\theta$ and $\cos\theta$ are plotted in Fig. 6 at times $t = 20$, 100 and 200. Note that in some region near the vortex the residual flow almost vanishes. This can also be seen from the asymptotics of ϕ_{res}. As $t \to \infty$ and for $r < |L|$ the results of Appendix B imply that near the vortex,

$$\phi_{\mathrm{res}} \approx \left[2I_1(r) - 2\frac{rI_1(a)}{a}\right]\exp\bigl(-|L|\bigr)\sin\theta + \mathrm{O}\left(\frac{\log^2 t}{t}\right). \tag{96}$$

The coefficient of $\sin\theta$ is small in practice. For example, for $a = 1$ and $L = 1.2$, the maximum modulus of ϕ_{res} in the interval $0 < r < |L|$ is approximately 0.021. The region in which ϕ_{res} is small grows with time. Reznik et al. [16] show that the residual flow for an intense β-plane vortex exhibits the same behaviour.

[5] And indeed of an intense singular vortex near an escarpment.

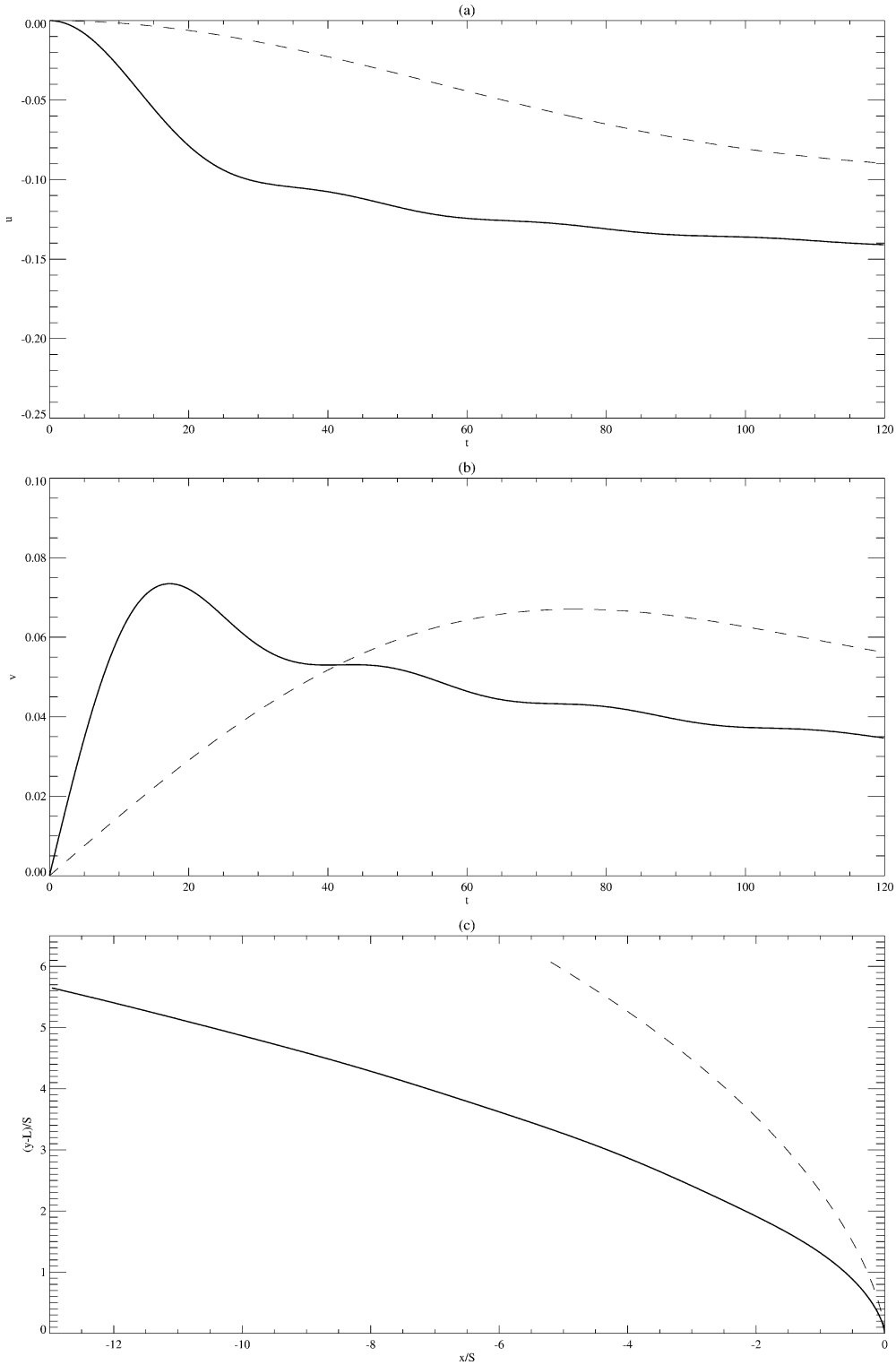

Fig. 4. The drift of an intense vortex patch near an escarpment. (a) Is a plot of the zonal drift velocity, (b) is a plot of the meridional drift velocity and (c) is a plot of the trajectory of the vortex centroid. The parameter values use are $L = 1.2$, $\alpha = -1$ (i.e., a cyclone), and $a = 1$ (solid line) and $a = 0.5$ (dashed line). See text for further comments.

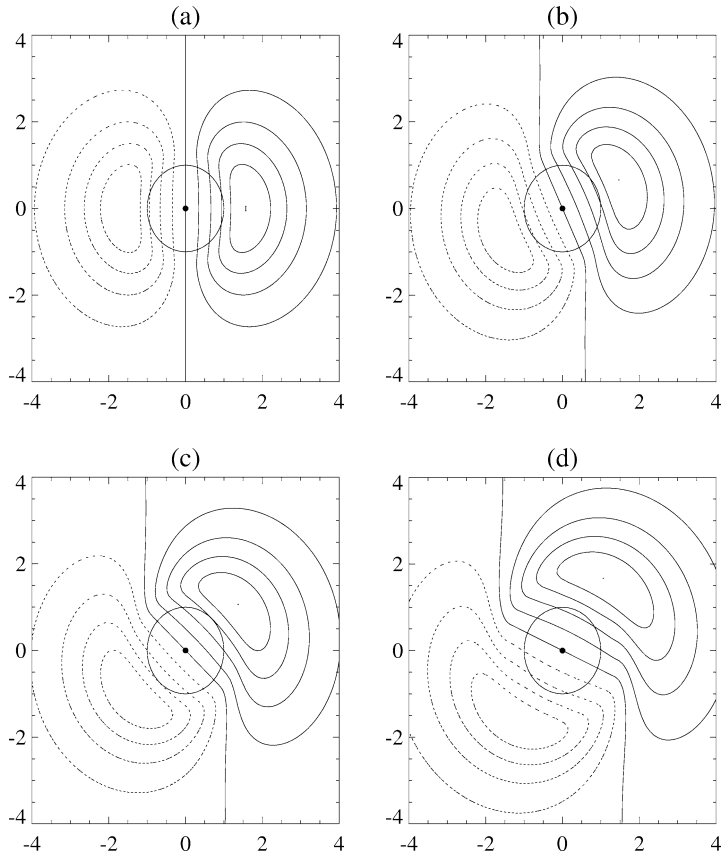

Fig. 5. Plots of the streamlines for the leading order solution, evaluated numerically by Eq. (83). The parameter values used are $a = 1$, $L = 1.2$ and $\alpha = -1$, i.e., a cyclone. The times are (a) $t = 0^+$, (b) $t = 10$, (c) $t = 20$ and (d) $t = 50$. See text for further comments.

Apart from explaining the leading order behaviour these asymptotic results reveal some of the features of the long time evolution of the vortex. Consider Eq. (73) describing the evolution of the second order vorticity correction q_2. The first Jacobian term in the right-hand side contains spatial derivatives of q_1. According to Eqs. (77), (78), for fixed r and θ, the radial derivative of q_1 consists of a term multiplied by $b'(r)t$ and a term which oscillates with t (the details are omitted). Hence the spatial derivatives of q_1 grow in time. This growth is confined to the vortex core, since $b'(r)$ decays rapidly away from the vortex. Near the vortex core, the the first term in the first Jacobian in (73) is approximated by (96). Since ϕ_{res} practically vanishes in the region near the vortex core, this Jacobian term grows only slowly with time. A similar argument applies for the second Jacobian in the right-hand side of (73). The right-hand side of (73) multiplied by S^2 is the next order term when substituting the leading order solution $\phi_0 + S\phi_1$ into the governing equation (7). Thus the leading order solution $\phi_0 + S\phi_1$ may describe the vortex evolution beyond $t = \mathrm{O}(S^{-1})$.

Eq. (73) may be rewritten

$$\frac{\partial q_2}{\partial t} + b(r)\frac{\partial q_2}{\partial \theta} = F(r,t) + G^{(s)}(r,t)\sin 2\theta + G^{(c)}(r,t)\cos 2\theta, \tag{97}$$

where F and $G^{(\nu)}$ depend on u_1 and v_1, and contain δ-functions. This implies that the second order term in the expansion of the regular streamfuncion, ϕ_2 consists of an axisymmetric component and a quadrupole component. In the study of Reznik et al. [16], it was found that the axisymmetric part of the second order vorticity correction for an intense vortex patch on the β-plane fills a growing region near the vortex centre, while the quadrupole component decays with time. This results in a growing region of axisymmetric flow, and the differential rotation, due to relative vorticity production in the growing annulus around the vortex serves to preserve the circular shape of the vortex. The vortex is contained in a 'trapped region', which is surrounded by a region of weaker potential vorticity. The differential rotation means that inside the trapped zone the flow is strongly axisymmetric, which prevents the deformation of the patch. The plausibility of this process in the present case is investigated numerically in Part II. It is worth noting that in the rigid-lid (non-divergent) limit, the slow decay of the velocity

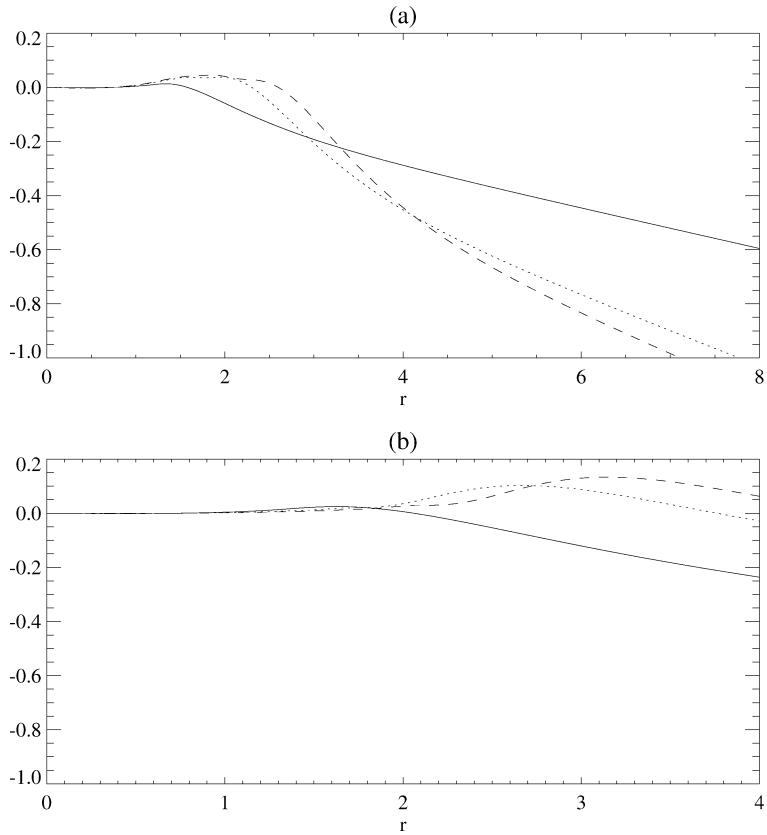

Fig. 6. The coefficients of $\sin\theta$ and $\cos\theta$ in Eq. (95): (a) the coefficient of $\sin\theta$ and (b) the coefficient of $\cos\theta$. The parameters used are $L = 1.2$, $a = 1$ and $\alpha = -1$ at times $t = 20$ (solid line), $t = 100$ (dotted line) and $t = 200$ (dashed line).

field in the far-field of the vortex means the situation will be very different. The trapping may not occur, and wave radiation might be important for all times. See Llewellyn-Smith [12].

Near the vortex centre, the solution $\psi_0 + S\phi_1$ tends to

$$\psi_\infty = \psi_0\big(\big((x + Su_1 t)^2 + y^2\big)^{1/2}\big) + Su_1 y, \tag{98}$$

where ψ_0 is the initial condition given in Eq. (21). In obtaining this solution, the approximation $I_1(r) \approx r/2$ for sufficiently small r has been used in (B.17).[6]. Reznik et al. [16] obtained a similar result for the leading order solution for an intense β-plane vortex. There is however a crucial difference with the present case. The steadily propagating vortex on the β-plane has westward drift velocity that precisely matches the Rossby long wave phase speed. The solution analogous to ψ_∞ is then an *exact* solution of the governing equation, and the authors are justified in saying that the nonlinearity "kills the β-effect", and the vortex adopts a non-radiating state. In the present case (98) is not a solution of (11). Moreover the vortex always travels with westward drift velocity of magnitude less than unity, i.e., at a velocity matching a possible phase speed of the topographic waves. Wave radiation must become important at large times. The large time behaviour is investigated by contour dynamics in Part II. Finally it is worth noting that the analysis of the intense vortex patch carried out here is more extensive that in the intense singular vortex case of McDonald [14] and, moreover, that much of the analysis performed here could equally well be applied in the singular vortex case.

[6] In practice $I_1(r) \approx r/2$ even for $r = 2$.

5. Conclusions

The leading order motion of an initially circular vortex patch near an escarpment has been derived, for the limits when the topographic vortex time scale is well separated from the advective time scale of the vortex. For a weak vortex, $S \gg 1$, it has been shown that the topographic waves rapidly propagate away from the vortex and have no leading order influence on the motion. For times which are short compared with T_w, the vortex remains circular, and the initial motion is south for anticyclones and north for cyclones. This initial motion is caused by the creation of a secondary dipole, formed by the vortex advecting fluid across the topographic gradient, and which thus gains relative vorticity. The initial disturbance is quickly propagated away from the vortex in the form of dispersive topographic waves, and the vortex begins to move as if the escarpment were a wall. This is the same behaviour as that of a weak singular vortex near an escarpment, and in the limit that the vortex is small compared with its distance from the escarpment the singular vortex results are recovered.

On the other hand for $S \ll 1$, the vortex is intense. To leading order in S the vortex also remains circular. The secondary circulations created by the vortex advecting fluid across the topographic gradient also initially cause anticyclones to move south, and cyclones to move north. However the strong axisymmetric swirl of the vortex prevents these initial disturbances from moving away from the vortex. The secondary dipole is rotated by the primary vortex, and consequently anticyclones follow a curved southwest trajectory, while cyclones move northwest. This is qualitatively the same mechanism as the β-gyres which lead to the characteristic paths of intense β-plane vortices. Further analytic progress is inhibited by the piecewise constant nature of the evolving relative vorticity distribution. However, several features of the dynamics appear to increase the axisymmetrisation of the flow near the vortex and point to the existence of a trapped region near the vortex. At large times wave radiation is likely to affect the structure of the vortex.

The results for both the weak and the intense vortices tend to those for weak and intense singular vortices in the limit that the patch is vanishingly small, and with large circulation near the centre – precisely the conditions under which the singular vortex is touted as a model for uniform vortex patch. Moreover the external structure of a vortex patch is the same as that of a singular vortex, and it might be expected that as long as the patch remains circular then a singular vortex model may describe the motion well.

In Part II the full range of vortex intensities will be investigated using the contour advection scheme of Dritschel [4]. It is of interest to investigate the validity of the analytic solutions obtained here. It is not anticipated that the weak vortex will remain circular, but the validity of the pseudoimage concept can be investigated by comparing the motion with that of an equivalent vortex near a wall. Of particular interest is the large time response of the vortex to topographic wave radiation. The intense vortex is expected to remain circular for longer times, and it is of interest to examine the large time behaviour and test the heuristic predictions made here.

In the remaining case of a moderate vortex ($S \approx 1$) no theory has been presented here. The contour advection scheme integrates the full nonlinear equations, and enables the full parameter space to be investigated. It is of interest to compare the behaviour of moderate vortices near an escarpment with moderate β-plane vortices (see the analytical and numerical study of Lam and Dritschel [11]) and with the behaviour of moderate barotropic vortices approaching an escarpment (see the experimental and numerical study of Zavala Sanson, van Heijst and Doorschoot [21]).

Appendix A. Derivation of the Fourier series coefficients for q_1

In this appendix the $m = 1$ Fourier series coefficients for q_1 in Section 5.3.1 are derived. First, for times $t < \mathrm{O}(S^{-1})$, the meridional drift velocity $v_1 = \mathrm{O}(S)$, so that $y_c = L + \mathrm{O}(S)$. Hence for $t < \mathrm{O}(S^{-1})$, Eq. (69) can be written

$$q_1 = \frac{1}{2}\left[\operatorname{sgn}\left(\sin\big(\theta - b(r)t\big) + \frac{L}{r}\right) - \operatorname{sgn}\left(\sin\theta + \frac{L}{r}\right)\right]. \tag{A.1}$$

Next note that if $r < |L|$ then $q_1 = 0$. For $r > |L|$ the constant term in the Fourier series for q_1 is

$$a_0 = \frac{1}{\pi}\int_{-\pi-bt}^{\pi-bt} \operatorname{sgn}\left(\sin\theta + \frac{L}{r}\right)\mathrm{d}\theta - \frac{1}{\pi}\int_{-\pi}^{\pi} \operatorname{sgn}\left(\sin\theta + \frac{L}{r}\right)\mathrm{d}\theta, \tag{A.2}$$

which vanishes, since the two integrands are periodic with period 2π, and the integrals are each over an interval of length 2π. Writing $q_1^{(c)}$ and $q_1^{(s)}$ for the coefficients of $\sin\theta$ and $\cos\theta$ leads to

$$q_1^{(s)}(r,t) = \frac{\cos bt - 1}{2\pi}\int_I \operatorname{sgn}\left(\sin\theta + \frac{L}{r}\right)\sin\theta\,\mathrm{d}\theta + \frac{\sin bt}{2\pi}\int_I \operatorname{sgn}\left(\sin\theta + \frac{L}{r}\right)\cos\theta\,\mathrm{d}\theta, \tag{A.3}$$

and

$$q_1^{(c)}(r,t) = \frac{\cos bt - 1}{2\pi} \int_I \operatorname{sgn}\left(\sin\theta + \frac{L}{r}\right)\cos\theta \,\mathrm{d}\theta - \frac{\sin bt}{2\pi} \int_I \operatorname{sgn}\left(\sin\theta + \frac{L}{r}\right)\sin\theta \,\mathrm{d}\theta, \tag{A.4}$$

where I is an interval of length 2π. Denote by θ_c the (two) values of θ in the interval I where the sgn function changes sign, i.e., $\sin\theta_c = -L/r$. By dividing the integrals into three intervals according to whether the sgn function is positive or negative it is straightforward to show, for $r > |L|$

$$\int_I \operatorname{sgn}\left(\sin\theta + \frac{L}{r}\right)\sin\theta \,\mathrm{d}\theta \;=\; 4|\cos\theta_c| = \frac{4}{r}\sqrt{r^2 - L^2}, \tag{A.5}$$

$$\int_I \operatorname{sgn}\left(\sin\theta + \frac{L}{r}\right)\cos\theta \,\mathrm{d}\theta \;=\; 0. \tag{A.6}$$

Hence, the required coefficients are,

$$q_1^{(s)} \;=\; \frac{2}{\pi r}\sqrt{r^2 - L^2}(\cos bt - 1), \tag{A.7}$$

$$q_1^{(c)} \;=\; -\frac{2}{\pi r}\sqrt{r^2 - L^2}\sin bt, \tag{A.8}$$

for $r > |L|$ and $q_1^{(s)} = q_1^{(c)} = 0$ otherwise.

Appendix B. Asymptotic results for drift velocity components for intense vortex

(a) Behaviour as $t \to 0$. Consider Eq. (89). For $t \ll 1$ approximate

$$1 - \cos(bt) \approx -\frac{(bt)^2}{2} = -\frac{\alpha^2 a^2 I_1^2(a) t^2}{2r^2} K_1^2(r), \quad r > a, \tag{B.1}$$

so that

$$u \approx -\frac{\alpha^2 a I_1^3(a) t^2}{2\pi} \int_L^\infty \frac{K_1^3(r)}{r^2}\sqrt{r^2 - L^2}\,\mathrm{d}r. \tag{B.2}$$

The integral converges and the integrand is positive definite for $L \leqslant r < \infty$. Hence the integral is a positive constant, say A, which depends on L, i.e.,

$$u \approx -\frac{A\alpha^2 a I_1^3(a)}{2\pi} t^2 \tag{B.3}$$

as $t \to 0$. Similarly, approximating

$$\sin(bt) \approx bt = -\frac{\alpha a I_1(a) t}{r} K_1(r), \tag{B.4}$$

in Eq. (90) for $t \ll 1$, leads to

$$v \approx -\frac{B\alpha I_1^2(a)}{\pi} t, \tag{B.5}$$

as $t \to 0$, where B is a positive constant which depends on L.

(b) Behaviour as $t \to \infty$. It is useful to approximate the large time behaviour of ϕ_1 in the near field of the vortex, from which the asymptotic drift velocity components can be deduced. Consider $\phi_1^{(s)}$, for $r < |L|$. From (83) this may be written

$$\phi_1^{(s)} = -\frac{2}{\pi} I_1(r)[P_1 + P_2 + P_3], \tag{B.6}$$

where

$$P_1 = -\int_L^\infty \sqrt{\rho^2 - L^2} K_1(\rho)\,\mathrm{d}\rho, \tag{B.7}$$

$$P_2 = \int_L^{r_1} \cos bt \sqrt{\rho^2 - L^2} K_1(\rho)\,\mathrm{d}\rho, \tag{B.8}$$

$$P_3 = \int_{r_1}^\infty \cos bt \sqrt{\rho^2 - L^2} K_1(\rho)\,\mathrm{d}\rho. \tag{B.9}$$

Here r_1 is large but fixed. First note that

$$P_1 = -\pi \exp\bigl(-|L|\bigr). \tag{B.10}$$

See, e.g., McDonald [14]. Next consider P_2. Write the angular velocity of the vortex

$$b(r) = -\Gamma \frac{K_1(r)}{r}, \tag{B.11}$$

where $\Gamma = \alpha a I_1(a)$. From Ambramowitz and Stegun [1] the derivative of $K_1(r)$ is

$$K_1'(r) = -K_2(r) + \frac{1}{r} K_1(r), \tag{B.12}$$

so that

$$b'(r) = \Gamma \frac{K_2(r)}{r}. \tag{B.13}$$

Hence $b'(\rho) \neq 0$ on the interval $L < \rho < r_1$. Moreover, $\sqrt{\rho^2 - L^2} K_1(\rho)$ is integrable on this interval. It then follows that,

$$P_2 = \mathrm{O}\bigl(t^{-1}\bigr), \tag{B.14}$$

as $t \to \infty$ (see [3, p. 278]). For $r_1 \gg L$ approximate $\sqrt{\rho^2 - L^2} \approx \rho$ and $K_n(\rho) \approx \mathrm{e}^{-\rho}/\sqrt{\rho}$ for $n = 1, 2$. Then

$$P_3 \approx \int_{r_1}^\infty \cos bt \rho K_1(\rho)\,\mathrm{d}\rho = \frac{1}{\Gamma} \int_{\xi_1}^0 \cos \xi t \rho^2 \frac{K_1(\rho)}{K_2(\rho)}\,\mathrm{d}\rho \approx \frac{1}{\Gamma} \int_0^{\xi_1} \cos \xi t \log^2 \xi\,\mathrm{d}\xi,$$

since for large ρ, $\xi \approx \mathrm{e}^{-\rho}$. Here $\xi_1 = |\Gamma| K_1(r_1)/r_1$. Making a further change of variable leads to

$$P_3 \approx \frac{1}{\Gamma t} \int_0^{\xi_1 t} \sin z \log^2\left(\frac{z}{t}\right) \mathrm{d}z. \tag{B.15}$$

Integration by parts implies that the leading order behaviour of the integral is $\mathrm{O}(\log^2 t)$ as $t \to \infty$. That is, for large t

$$P_3 = \mathrm{O}\left(\frac{\log^2 t}{t}\right). \tag{B.16}$$

Hence it follows that

$$\phi_1^{(s)} = 2 I_1(r) \exp\bigl(-|L|\bigr) + \mathrm{O}\left(\frac{\log^2 t}{t}\right), \tag{B.17}$$

as $t \to \infty$. A similar treatment for the component $\phi_1^{(c)}$ leads to

$$\phi_1^{(c)} = \mathrm{O}\left(\frac{\log^2 t}{t}\right), \tag{B.18}$$

as $t \to \infty$. Finally the vortex drift velocity components may be obtained from (89), (90), (B.17) and (B.18) and are

$$u_1 \approx -\frac{2 I_1(a)}{a} \exp\bigl(-|L|\bigr) + \mathrm{O}\left(\frac{\log^2 t}{t}\right), \tag{B.19}$$

$$v_1 \approx \mathrm{O}\left(\frac{\log^2 t}{t}\right). \tag{B.20}$$

References

[1] M. Ambramowitz, I.A. Stegun, Handbook of Mathematical Functions, Dover, 1972.
[2] J.D. Beismann, R.H. Käse, J.R.E. Lutejeharms, On the influence of submarine ridges on translation and stability of agulhas rings, J. Geophys. Res. 104 (C4) (1991) 7897–7906.
[3] C.M. Bender, S.A. Orszag, Advanced Mathematical Methods for Scientists and Engineers, McGraw-Hill, 1978.
[4] D.G. Dritschel, Contour surgery: a topological reconnection scheme for extended integrations using contour dynamics, J. Comput. Phys. 77 (1988) 240–266.
[5] D.G. Dritschel, M.H.P. Ambaum, A contour-advective semi-Lagrangian numerical algorithm for simulating fine-scale conservative dynamical fields, Q. J. R. Met. Soc. 123 (1997) 1097–1130.
[6] D.C. Dunn, The motion of an initially circular vortex near an escarpment. Part II: numerical results, J. Eur. Mech. B Fluids (2002), submitted.
[7] D.C. Dunn, N.R. McDonald, E.R. Johnson, The motion of a singular vortex near an escarpment, J. Fluid Mech. 448 (2001) 335–365.
[8] I.S. Gradshteyn, I.M. Rhyzik, Tables of Integrals Series and Products, Academic Press, 1980.
[9] E.R. Johnson, Starting flow for an obstacle moving transversely in a rapidly rotating fluid, J. Fluid Mech. 149 (1984) 71–88.
[10] E.R. Johnson, M.K. Davey, Free-surface adjustment and topographic waves in coastal currents, J. Fluid Mech. 219 (1990) 273–289.
[11] J.S.-L. Lam, D.G. Dritschel, On the beta-drift of an initially circular vortex patch, J. Fluid Mech. 436 (2001) 107–129.
[12] S.G. Llewellyn-Smith, The motion of a non-isolated vortex on the beta-plane, J. Fluid Mech. 346 (1997) 149–179.
[13] N.R. McDonald, Topographic dispersal of bottom water, J. Phys. Ocean. 23 (1992) 954–969.
[14] N.R. McDonald, Motion of an intense vortex near topography, J. Fluid Mech. 367 (1998) 359–377.
[15] R.T. Pierrehumbert, A family of steady, translating vortex pairs with distributed vorticity, J. Fluid Mech. 99 (1980) 129–144.
[16] G.M. Reznik, R. Grimshaw, E.S. Benilov, On the long term evolution of an intense localised divergent vortex on the β-plane, J. Fluid Mech. 422 (1998) 249–280.
[17] P.L. Richardson, A. Tychensky, Meddy trajectories in the canary basin, J. Geophys. Res. 103 (1998) 25029–25045.
[18] M.E. Stern, Scattering of an eddy advected by a current towards a topographic obstable, J. Fluid Mech. 402 (2000) 211–223.
[19] G.G. Sutyrin, G.R. Flierl, Intense vortex motion on the beta plane: development of the beta gyres, J. Atmos. Sci. 51 (1994) 773–790.
[20] G.B. Whitham, Linear and Nonlinear Waves, Wiley, 1974.
[21] I. Zavala Sanson, G.J.F. van Heijst, J.J.J. Doorschoot, Reflection of barotropic vortices from a step-like topography, Nuovo Cimento C 22 (2000) 909–930.